THERMOCAPILLARY FLOWS WITH LOW FREQUENCY g-JITTER

P. Grassia, G.M. Homsy, *Department of Chemical Engineering, Stanford CA 94305-5025, USA.*
bud@chemeng.stanford.edu

ABSTRACT

A thermocapillary parallel flow is established in a fluid filled slot with an applied temperature gradient. Low frequency jitter is imposed in arbitrary directions. Vertical jitter proves to be relatively uninteresting, merely augmenting or opposing the basic thermocapillary flow. Streamwise jitter still produces parallel flows, but these now exhibit boundary layers or layered cellular structures for large Rayleigh number as the applied stratification alternates between stable and unstable. Runaways are possible for unstable stratification and these correspond to resonant excitation of stationary long wave Rayleigh-Bénard modes. Spanwise jitter produces fully three dimensional motion. A spanwise-streamwise circulation results for weak spanwise jitter, which advects the interfacial temperature establishing a subsidiary spanwise thermocapillary flow. This flow is strong at small Biot number when advected temperature is trapped in the slot, and has a counter-intuitive dependence on the spanwise-streamwise aspect ratio.

1 INTRODUCTION

Materials processing situations frequently involve interfaces with lengthwise temperature gradients, and are therefore susceptible to thermocapillary motions. If materials processing is conducted in space, the thermocapillary flows will also be subject to fluctuating accelerations (g-jitter) characteristic of the space based microgravity environment [1, 2, 3, 4]. While there has been a large number of studies of buoyant systems subject to gravitational modulation [5, 6, 7, 8, 9, 10], there is no equivalent body of results for thermocapillary systems under these circumstances.

The present paper considers the effect of jitter on a basic thermocapillary flow in a particularly simple geometry: a fluid layer of finite depth but infinite horizontal extent. This is the thermocapillary slot flow of Davis and coworkers [11, 12], which is sketched in Figure 1. The underlying simplicity of the slot model is such that, even when jitter is added, the problem remains amenable to analytical techniques. This permits a thorough parametric study of the system, allowing the possibility of considering several different directions of jitter, including spanwise jitter which has been little studied to date even for buoyancy driven flows. The structure of the paper is as follows. In the next section we introduce the governing equations of the slot. In §3 we present results for jitter confined to the plane, and in §4 we consider spanwise jitter. Conclusions are given in §5. Full details may be found elsewhere [13, 14].

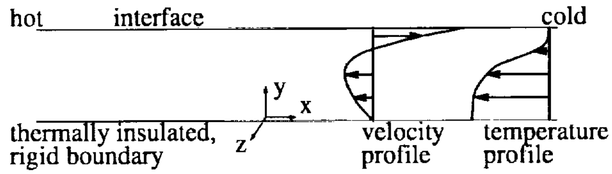

Figure 1: Thermocapillary slot return flow produced by a lengthwise applied temperature gradient. A vertically varying advected temperature profile, which balances streamwise heat convection and vertical heat conduction, is also present.

2 GOVERNING EQUATIONS

The governing continuity, momentum and thermal equations of the slot subject to g-jitter are

$$\begin{aligned} \nabla.\mathbf{u} &= 0, & (1)\\ MaPr^{-1}(\mathbf{u}_{,t}+\mathbf{u}.\nabla\mathbf{u}) &= -\nabla p+\nabla^2\mathbf{u}+\mathbf{G}T, & (2)\\ Ma(T_{,t}+\mathbf{u}.\nabla T) &= \nabla^2 T, & (3)\end{aligned}$$

where Ma is the Marangoni number, Pr is the Prandtl number and $\mathbf{G}$ represents the dimensionless jitter, consisting of a dynamic Bond number G, multiplied by an $O(1)$ vector describing the direction and time modulation of gravity. Note that the momentum equation can be recast as a vorticity equation

$$Re(\boldsymbol{\omega}_{,t}+\mathbf{u}.\nabla\boldsymbol{\omega}) = Re\boldsymbol{\omega}.\nabla\mathbf{u}+\nabla^2\boldsymbol{\omega}+\nabla T\times\mathbf{G}, \quad (4)$$

which clearly shows the role of temperature gradients in vorticity generation. The temperature field is most conveniently written $T=-x+T^a(x,y,z,t)$ where $-x$ represents the applied temperature field, that is responsible for the basic thermocapillary flow, and T^a is produced by advection.

The base of the slot $y=0$ is an inpenetrable, no slip, thermally insulated boundary. The interface $y=1$ is assumed to remain flat, to sustain thermocapillary stresses, and to permit heat transfer characterized by a Biot number Bi. Accordingly

$$\begin{aligned} \mathbf{u}=T^a_{,y} &= 0 \text{ at } y=0 \text{ and}\\ v=u_{,y}-1+T^a_{,x}=w_{,y}+T^a_{,z} & \\ =T^a_{,y}+BiT^a &= 0 \text{ at } y=1. \quad (5)\end{aligned}$$

The slot flows must also be consistent with no fluid penetration conditions which would apply on the sidewalls of a cavity of finite extent. There are various ways of ensuring this, depending on the class of slot flow. In many cases return flow conditions will apply

$$\int_0^1 u\,dy = \int_0^1 w\,dy = 0. \qquad (6)$$

However there are also more general possibilities (to be discussed in §4).

In the absence of jitter $\mathbf{G} = 0$ the equations admit parallel flow solutions in the x direction, with the advected temperature field varying only in the vertical. The solutions are [11, 12]

$$u = \tfrac{3}{4}y^2 - \tfrac{1}{2}y, \quad T^a = -\tfrac{1}{48}Ma(3y^4 - 4y^3 + 1). \qquad (7)$$

Our goal is to calculate how these solutions are modified in the presence of jitter. For simplicity we assume throughout that the modulation occurs at some frequency Ω which is small enough to be quasistatic, allowing the neglect of time derivatives in equations (2)–(3).

3 JITTER WITHIN THE PLANE

If $\mathbf{G}$ is non-zero but confined to the xy plane, we still obtain parallel flow solutions, with advected temperature varying only in the vertical. It is clear from equation (4) that *vertical* components of gravity only produce vorticity when coupled to the applied temperature field, not when coupled to T^a. As the applied temperature is independent of any thermocapillary motion, thermocapillarity and vertical gravity operate independently of one another. If $\mathbf{G} = (0, G\cos\Omega t, 0)$ vertical gravity produces fields

$$\begin{aligned} u &= -\tfrac{1}{24}G\cos\Omega t\left(4y^3 - \tfrac{15}{2}y^2 + 3y\right), \\ T^a &= \tfrac{1}{24}Ma\,G\cos\Omega t\left(\tfrac{1}{5}y^5 - \tfrac{5}{8}y^4 + \tfrac{1}{2}y^3 - \tfrac{3}{40}\right), \end{aligned} \qquad (8)$$

additional to those of equation (7). Thus vertical gravity alternately cooperates or competes with the thermocapillary fields as $G\cos\Omega t$ executes its oscillation cycle.

Now consider the case of *streamwise* gravity given by $\mathbf{G} = (G\cos\Omega t, 0, 0)$. From equation (4) we deduce that this generates vorticity when coupled with the advected temperature field, implying an interaction will occur between thermocapillarity and streamwise gravity. We define a streamfunction ψ such that $u = \psi_{,y}$. The thermal equation (3) now relates the streamwise heat advection $Ma\,\psi$ and the vertical heat conduction $-T^a_{,y}$. Substituting into vorticity equation (4), we deduce

$$\psi_{,yyyy} - Ra\cos\Omega t\,\psi = 0, \qquad (9)$$

where the Rayleigh number Ra equals $Ma\,G$. The boundary conditions are $\psi = \psi_{,y} = 0$ at $y = 0$, and $\psi = \psi_{,yy} - 1 = 0$ at $y = 1$.

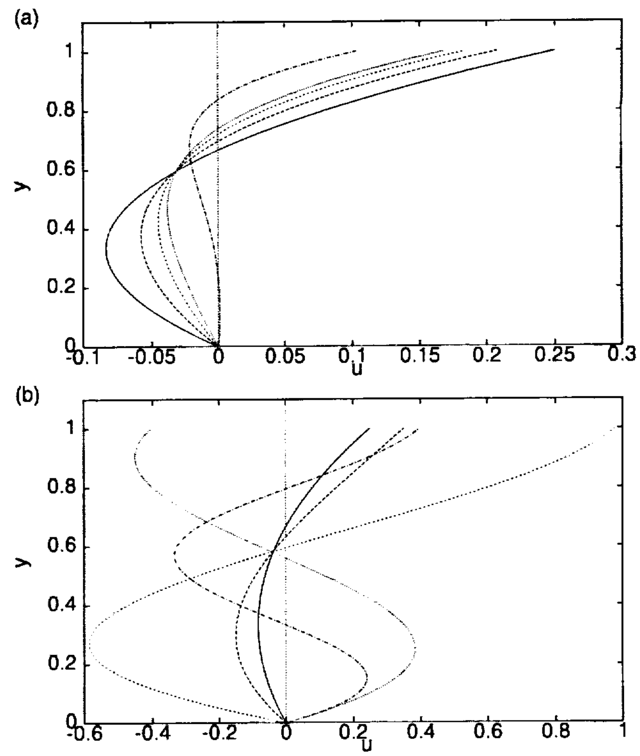

Figure 2: Velocity profiles for streamwise jitter during the (a) stable and (b) unstable part of the oscillation cycle, with solid line: $Ra|\cos\Omega t| = 0$, the base state profile; long dashes: $Ra|\cos\Omega t| = 100$; short dashes: $Ra|\cos\Omega t| = 200$; and dash-dot line: $Ra|\cos\Omega t| = 2200$. As $Ra|\cos\Omega t|$ increases, the stable case (a) tends to form an interfacial boundary layer, while the unstable case (b) forms cellular structures. Additionally in (b), the profiles obtain a large amplitude if they lie near one of the runaway values of $Ra\cos\Omega t$.

The solutions of this equation will be linear combinations of trigonometric and exponential functions. However these solutions are structurally quite different depending on the sign of $Ra\cos\Omega t$. If $Ra\cos\Omega t$ is large and negative, the solutions tend to be confined in boundary layers (see Figure 2(a)). If $Ra\cos\Omega t$ is large and positive, the solutions are highly cellular in nature (see Figure 2(b)). In both cases the thickness of the boundary layers or the wavelength of the cells scales as $\left(Ra|\cos\Omega t|\right)^{-1/4}$. There are also found to be particular positive values of $Ra\cos\Omega t$ which lead to infinitely large responses or runaways.

Physical insights into the reason for the different behaviour in the two cases can be deduced by considering the stratified slot initially in the absence of thermocapillarity. If $Ra\cos\Omega t < 0$, gravity and the applied temperature gradient are anti-parallel, meaning the slot is stably stratified in the

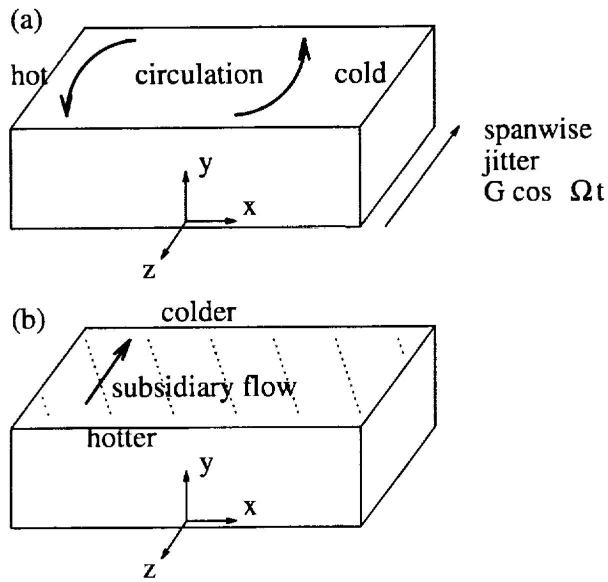

Figure 3: (a) Purely buoyant circulation flow induced by spanwise jitter in a slot with an applied temperature gradient. The circulation alternates between anticlockwise and clockwise as the jitter proceeds. (b) The circulation convects heat and rotates the isotherms (shown as dotted lines). The presence of a non-zero spanwise component of the interfacial temperature gradient drives a subsidiary thermocapillary flow.

Rayleigh-Bénard sense. If $Ra\cos\Omega t > 0$, gravity and the applied temperature gradient become parallel, corresponding to unstable stratification. If thermocapillarity is now added to the stably or unstably stratified system, it breaks the symmetry of the Rayleigh-Bénard basic state, thereby imposing directionality on the flow. The runaways in the unstable case correspond to values of the quasistatic Rayleigh number $Ra\cos\Omega t$ that support stationary, long wave Rayleigh-Bénard modes, which become resonantly excited by the thermocapillary forcing.

4 SPANWISE JITTER

If $\mathbf{G} = (0, 0, G\cos\Omega t)$ equations (1)–(5) no longer admit parallel flow solutions, and in fact a non-linear set of equations must be solved and the flows are fully 3-dimensional. For weak spanwise jitter, we pursue a perturbation expansion in powers of $G\cos\Omega t$. It is clear from equation (4) that spanwise jitter coupling to the applied temperature field generates vertical vorticity at leading order. This produces a purely buoyant circulation flow around the slot (see Figure 3(a)). We concentrate solely on the leading order results here. Results through second order, which necessarily include steady streaming flows, are given in [14].

In determining this circulation, we want to continue to exploit the horizontal spatial invariance properties that follow from the geometric simplicity of the slot model. Accordingly we assume a first order circulation flow of the form $G\cos\Omega t\,(zu_{01}(y), 0, xw_{10}(y))$ where u_{01} and w_{10} are functions to be determined. These functions are necessarily non-return flows, and in place of equation (6) we do the following. Imagine that the infinite slot models a true shallow cavity of unit depth, length A^{-1} and breadth $A_{zx}A^{-1}$. Consider a quadrant $0 \le x \le \frac{1}{2}A^{-1}, 0 \le z \le \frac{1}{2}A_{zx}A^{-1}$, located between the cavity centre and one corner. No penetration conditions on the cavity sidewalls require that the fluid flux entering the quadrant along $x = 0$ matches that leaving along $z = 0$. Applied to the assumed slot flows this requires

$$\int_0^1 w_{10}\,dy = -A_{zx}^2 \int_0^1 u_{01}\,dy. \tag{10}$$

The parameter A has cancelled from equation (10) but the spanwise-streamwise aspect ratio A_{zx} must be retained. The solutions for u_{01} and w_{01} are found to be

$$u_{01} = -\frac{1}{1+A_{zx}^2}\left(\tfrac{1}{2}y^2 - y\right), \tag{11}$$

$$w_{10} = \frac{A_{zx}^2}{1+A_{zx}^2}\left(\tfrac{1}{2}y^2 - y\right). \tag{12}$$

Clearly streamwise (spanwise) circulation flow is favoured at small (large) A_{zx}.

The circulation flow convects heat and therefore rotates the isotherms. This produces a temperature $G\cos\Omega t\, zT_{01}(y)$ where

$$T_{01} = \frac{Ma}{1+A_{zx}^2}\left(\tfrac{1}{24}y^4 - \tfrac{1}{6}y^3 + \tfrac{1}{8} + \frac{1}{3Bi}\right). \tag{13}$$

The term involving Bi accounts for the interfacial value of T_{01} and tends to be dominant even for Bi values as large as unity. A non-zero interfacial advected temperature arises here because the circulations are not return flows, and hence convect heat along the layer. If $Bi \to 0$ the convected heat has great difficulty escaping the interface, and so the temperature in the slot rises to a very high level.

As there are now additional temperature gradients along the surface in excess of the applied temperature gradient, new subsidiary thermocapillary motions are produced (see Figure 3(b)). These will be in the spanwise direction and we write them as $G\cos\Omega t\, w_{00}(y)$, where

$$w_{00} = \frac{Ma}{(1+A_{zx}^2)Bi}\left(\tfrac{1}{6}y - \tfrac{1}{4}y^2\right). \tag{14}$$

If thermocapillarity is inherently strong (Ma is large) or if heat is trapped in the slot (Bi is small) the subsidiary flow can dominate the circulation. The parametric dependence of

w_{00} on A_{zx} is counterintuitive on geometric grounds, i.e. the spanwise subsidiary flow is largest when spanwise-streamwise A_{zx} aspect ratio is small. The reason is that small A_{zx} favours the streamwise circulation that produces the isotherm rotation which in turn drives w_{00}.

5 CONCLUSIONS

The thermocapillary slot model subject to g-jitter exhibits rich physical behaviour. The simplicity of the slot geometry allows an analytic approach to the problem, facilitating a thorough parametric investigation, including the possibility of considering various directions of jitter. Vertical jitter is uninteresting because the advected temperature fields that are produced do not themselves produce any vorticity. Streamwise jitter is more interesting, and produces velocity profiles exhibiting boundary layer structures in the stable part of the cycle and cells in the unstable part. In the latter case it is possible to resonantly excite stationary long wave Rayleigh-Bénard modes for particular values of the quasistatic Rayleigh number. Spanwise jitter generates circulation flows around the slot. As the circulation advects interfacial temperature, it establishes subsidiary spanwise thermocapillary flows. At large Marangoni number or small Biot number, these subsidiary motions can become important.

ACKNOWLEDEMENTS

The authors acknowledge the support of NASA Grants NAG3-1475-S1 and NAG3-1943.

REFERENCES

[1] Alexander, J.I.D. 1990 *Low gravity experiment sensitivity to residual acceleration: A review.* Micrograv. Sci. Technol. **III**(2), 52–68.

[2] Nelson, E.S. 1991 *An examination of anticipated g-jitter on a space station and its effects on materials processing.* NASA Technical Memorandum 103775.

[3] Alexander, J.I.D., Lizée, A., Favier, J.-J. & Garandet, J.-P. 1996 *Analysis of residual acceleration effects on transport and segregation during directional solidification of tin-bismuth in the MEPHISTO furnace facility.* Third Microgravity Fluid Physics Conference, NASA Conference Publication **3338**, 461–464.

[4] Thomson, J.R., Drolet, F. & Viñals, J. 1996 *Fluid physics in a fluctuating acceleration environment.* Third Microgravity Fluid Physics Conference, NASA Conference Publication **3338**, 429–434.

[5] Gresho, P.M. & Sani, R.L. 1970 *The effects of gravity modulation on the stability of a heated fluid layer.* J. Fluid Mech. **40**, 783–806.

[6] Biringen, S. & Danabasoglu, G. 1990 *Computation of convective flow with gravity modulation in rectangular cavities.* J. Thermophysics **4**, 357–365.

[7] Biringen, S. & Peltier, L.J. 1990 *Numerical simulation of 3-D Bénard convection with gravitational modulation.* Phys. Fluids A **2**, 754–764.

[8] Farooq, A. & Homsy, G.M. 1994 *Streaming flows due to g-jitter-induced natural convection.* J. Fluid Mech. **271**, 351–378.

[9] Farooq, A. & Homsy, G.M. 1996 *Linear and non-linear dynamics of a differentially heated slot under gravity modulation.* J. Fluid Mech. **313**, 1–38.

[10] Lizée, A. & Alexander, J.I.D. 1997 *Chaotic thermovibrational flow in a laterally heated cavity.* manuscript.

[11] Sen, A.K. & Davis, S.H. 1982 *Steady thermocapillary flows in two-dimensional slots.* J. Fluid Mech. **121**, 163–186.

[12] Smith, M.K. & Davis, S.H. 1983 *Instabilities of dynamic thermocapillary liquid layers. Part 1. Convective instabilities.* J. Fluid Mech. **132**, 119–144.

[13] Grassia, P. & Homsy, G.M. 1998 *Thermocapillary & buoyant flows with low frequency jitter. Part I. Jitter confined to the plane.* Accepted for publication in Phys. Fluids.

[14] Grassia, P. & Homsy, G.M. 1998 *Thermocapillary & buoyant flows with low frequency jitter. Part II. Spanwise jitter.* Accepted for publication in Phys. Fluids.